

Extraction of correct Schottky barrier height of sulfur implanted NiSi/n-Si junctions: Junction doping rather than barrier height lowering

J. Chan,^{1,a)} N. Y. Martinez,¹ J. J. D. Fitzgerald,¹ A. V. Walker,¹ R. A. Chapman,¹ D. Riley,² A. Jain,² C. L. Hinkle,¹ and E. M. Vogel¹

¹Department of Materials Science and Engineering, The University of Texas at Dallas, Richardson, Texas 75080, USA

²Advanced CMOS, Texas Instruments Incorporated, Dallas, Texas 75243, USA

(Received 11 May 2011; accepted 21 June 2011; published online 8 July 2011)

Proper analysis of the Schottky barrier height extraction methods shows that sulfur implantation followed by anneal *does not* effectively reduce the Schottky barrier height of NiSi/n-Si contacts. Instead, the results for sulfur implanted samples are consistent with enhanced field emission due to an increased doping density of the surface region of the silicon. Sulfur has a large impact on contact resistivity for silicon with low initial doping concentration ($\lesssim 10^{17} \text{ cm}^{-3}$), but little impact for silicon with high initial doping density ($\gtrsim 10^{17} \text{ cm}^{-3}$). Internal photoemission measurements show that the Schottky barrier height remains unchanged with sulfur implantation. © 2011 American Institute of Physics. [doi:10.1063/1.3609874]

Reducing the specific contact resistivity of metal silicides on silicon can be achieved by increasing the junction dopant density or by reducing the Schottky barrier height (SBH) of the metal silicide.¹ Since the dopant density in the source/drain regions is close to solubility limits, it becomes increasingly important to reduce the SBH in order to achieve low contact resistivity. Implantation/segregation of various species has been extensively reported to reduce SBH in NiSi/Si contacts.^{2–7}

Schottky barrier diodes were fabricated on n-type, phosphorous-doped Si of various junction dopant densities: lightly doped ($\sim 2 \times 10^{15} \text{ cm}^{-3}$), moderately doped ($\sim 5 \times 10^{17} \text{ cm}^{-3}$), and degenerately doped ($\sim 1 \times 10^{20} \text{ cm}^{-3}$). Active regions were defined on 300 nm thermal SiO₂. Sulfur ions were implanted in the Si substrates at 5 keV with doses of 1×10^{13} , 5×10^{13} , and $3 \times 10^{14} \text{ cm}^{-2}$. Control samples without S implantation were also fabricated to complete the experimental matrix. The native oxide was removed from the active region using HF prior to radio frequency (RF) sputtering of 20 nm of Ni. NiSi was formed by a rapid thermal anneal (RTA) at 450°C for 30 sec in N₂. The unreacted Ni was selectively etched by Aqua Regia. Finally, Al was sputtered as a back contact. X-ray diffraction (XRD) confirmed that nickel-mono-silicide (NiSi) is formed in all samples. Current-voltage (*I-V*) data were measured at temperatures ranging from 270 K to 460 K, as shown in Figure 1. The reverse current increases with S implantation doses. The focus of this letter is to establish that the increase in the reverse current is due to enhanced tunneling current, rather than the lowering of the SBH.

The Arrhenius plots, i.e., $\ln(J/T^2)$ vs T^{-1} , obtained using 0.5 V reverse bias are shown in Figure 2(a). The SBH can be accurately obtained from the slope of the Arrhenius plots if the transport process is dominated by thermionic emission (TE). Figure 2(b) shows SBH obtained by fitting the *I-V* data with the TE equation:¹

$$J = A^{**} e^{\frac{-q\phi_b}{kT}} \left(e^{\frac{-qV_r}{nkT}} - 1 \right) \quad (1)$$

where *J* is the current density, *V_r* is the reverse bias, *n* is the ideality factor, and *A^{**}* is the Richardson constant. The lightly doped sample *without* S implantation shows a SBH of $\sim 0.68 \text{ eV}$, which is independent of temperature and agrees well with the accepted values.^{8–10} The SBH for this sample obtained from the Arrhenius plot, internal photoemission (IPE), and the capacitance-voltage (*C-V*) data (Table I) is almost identical.

For the *moderately* doped Si diode without S implantation, it is observed that the SBH obtained from the Arrhenius plot using TE is $\sim -0.02 \text{ eV}$, and the apparent SBH extracted using TE theory from the *I-V* data varies with temperature. The SBH measured for this sample using IPE and *C-V*, which are not dependent on the emission process, is $\sim 0.65 \text{ eV}$. The intrinsic SBH should not change significantly as a function of doping. The deviation of the SBH extracted from the Arrhenius plot is due to an increase in tunneling current, i.e., thermionic field emission (TFE). Arrhenius plots and

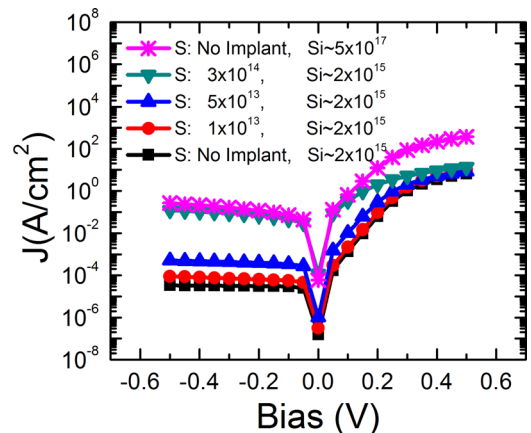


FIG. 1. (Color online) *I-V* characteristics of Schottky diode with different S doses (cm^{-2}) for $2 \times 10^{15} \text{ cm}^{-3}$ Si, and $5 \times 10^{17} \text{ cm}^{-3}$ Si with no S implant. Reverse current increases with S dose.

^{a)}Electronic mail: jack.chan@utdallas.edu.

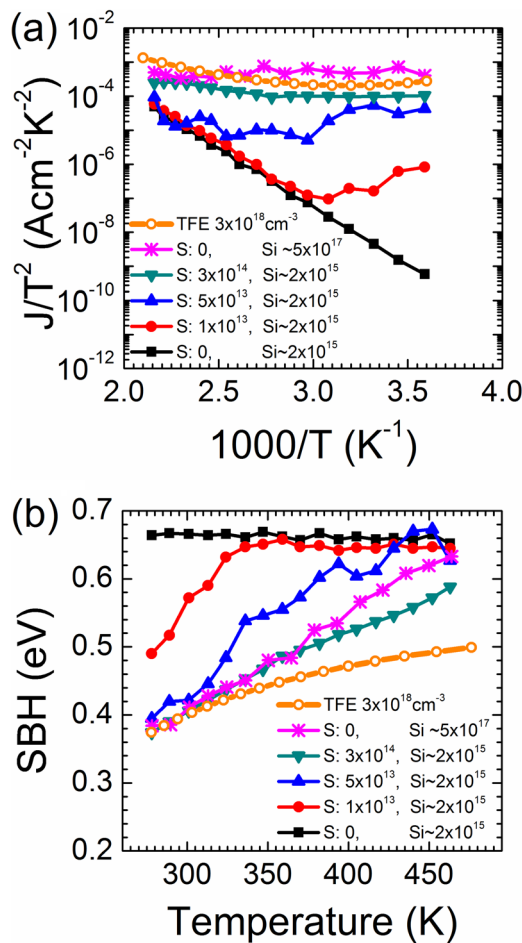


FIG. 2. (Color online) (a) Arrhenius plot and (b) SBH as a function of temperature, extracted under 0.5 V reverse bias for different S doses (cm⁻²) and Si dopant densities (cm⁻³). A calculation based on TFE equation with dopant density 3×10^{18} cm⁻³ is also shown for comparison.

apparent SBH data as a function of temperature are calculated using the TFE equation:¹

$$J = \frac{A^{**}T}{k} \sqrt{\pi E_{00}q} \left[V_r + \frac{\phi_b}{\cosh^2(E_{00}/kT)} \right] e^{-\frac{q\phi_b}{E_0}} e^{\frac{qV_r}{E'}}, \quad (2)$$

where $E_{00} = \frac{qh}{4\pi} \sqrt{\frac{N}{m^* \epsilon_s}}$, $E_0 = E_{00} \coth(E_{00}/kT)$, and $E' = \frac{E_{00}}{(E_{00}/kT) - \tanh(E_{00}/kT)}$, capture the major features in the Schottky diode data for higher doping density: (i) slopes in the Arrhenius plot becomes less negative as dopant density increases, which translates to a smaller extracted SBH and

(ii) the apparent SBH extracted from the I - V data using TE is smaller at lower temperatures. The lightly doped diode with the *highest* S dose shows a similar Arrhenius plot to the calculated TFE curves and a temperature dependent SBH. However, the corresponding SBH measured using IPE and C - V are 0.65 eV and 0.58 eV, respectively, as shown in Figure 3. It should be noted that all dopant densities extracted from the slope of the $1/C^2$ - V measurement (with and without S) are approximately 2×10^{15} cm⁻³. This is because under reverse bias, the C - V measures the dopant density at the depletion region edge which is >100 nm away from the junction interface, much further than the effective doping due to S implantation. The SBH measured using C - V is governed by the charge density in the depletion region, which is not significantly reduced due to tunneling in the junction interface as measured by the I - V method.

Another important point concerns the measurement temperature. The TE equation is accurate if kT is smaller than $1/3$ of the SBH.¹¹ In many studies, the SBH was reported to be ~ 0.1 eV after S implant, extracted from Arrhenius data measured below room temperature. However, it is more appropriate to measure the SBH at higher temperature if the transport is TFE. At higher temperatures, transport is due primarily to TE, and at lower temperatures the transport is dominated by TFE. The apparent SBH of the lightly doped diode with 1×10^{13} cm⁻² S remains at ~ 0.65 eV (Figure 2(b)) for temperatures > 350 K and starts to drop below 350 K. The Arrhenius plot extracts the correct SBH only if $T > 350$ K ($T^{-1} < 2.8 \times 10^{-3}$ K⁻¹) (Figure 2(a)), at which the SBH remains at ~ 0.67 eV. Using the low temperature regime of the Arrhenius plot significantly underestimates the SBH in S implanted NiSi/n-Si diodes.

The SIMS depth profile of S shows a peak concentration of $\sim 10^{18}$ – 10^{20} cm⁻³ at the NiSi/Si junction (Figure 4(a)). The depth profile of the P doping (not shown) is not affected by the S implant. Time-of-flight SIMS (Figure 4(b)) at a S dose of 3×10^{14} cm⁻² shows that the intensity of the SiS⁻ cluster ion is high, indicating that the Si and S are bound to each other. Since both the NiSiS⁺ and NiS⁻ ion intensities are negligibly small, it seems likely that these SiS⁻ cluster ions arise from the NiSi/Si interface or the Si substrate, instead of the NiSi layer. This is consistent with enhanced tunneling due to an increased dopant density in the TFE equation (and not for TE) and is further suggestive of S increasing the effective junction doping. Using the interfacial S density of 3 – 8×10^{19} cm⁻³ for the 2×10^{15} cm⁻³ doped Si and donor level of 0.32 eV (page 23 of Ref. 1) from the

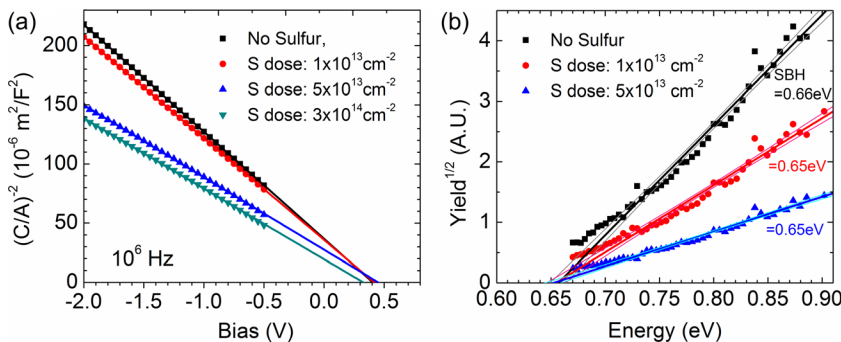


FIG. 3. (Color online) (a) Capacitance-voltage (C - V) measurement and (b) internal photoemission measurements for the Schottky diodes with Si dopant density 2×10^{15} cm⁻³. The extracted SBH is shown in Table I. SBH is not a strong function of S dose. SBH is extracted by fitting the IPE data from 0.70 eV to 0.90 eV, the 95% confident levels are also shown.

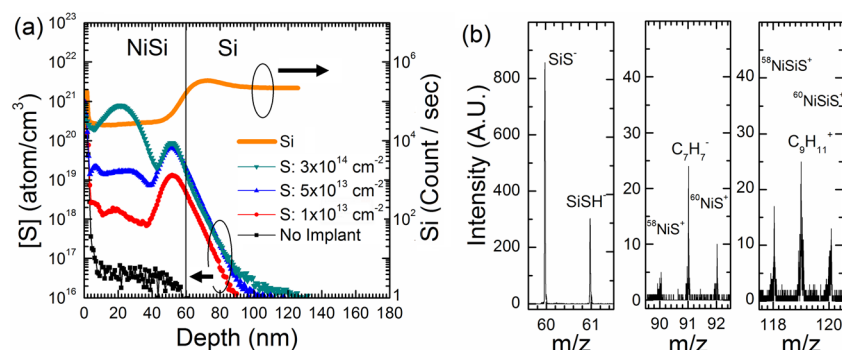


FIG. 4. (Color online) (a) A SIMS depth profile of S-implanted NiSi/Si which shows S concentrations of $\sim 10^{18}$ – 10^{20} cm⁻³ at the NiSi/Si interface (defined at the depth value corresponding to 50% of the rise in Si concentration signal). (b) Time-of-flight SIMS shows the prevalence of SiS⁻ clusters, but not Ni-S⁺ or NiSi-S⁺ clusters at a S dose of 3×10^{14} cm⁻².

conduction band, the ionized donor concentration, N_D^+ , calculated using charge balance under equilibrium at room temperature, is $\sim 1 \times 10^{17}$ cm⁻³. This additional S will raise the dopant density of the lightly doped diode into the TFE regime. It has also been shown that double donor levels may be introduced in Si by S.^{12,13} The activation process for S during the 450°C silicidation must still be identified. However, the diffusion of Ni during silicidation could open a pathway for substitutional bonding of S to Si as suggested by the SIMS data. It is well known that tunneling leads to a reduction in contact resistance.¹ We measured the specific contact resistivity, ρ_c , as a function of S dose at room temperature under reverse bias (not shown). Implantation of S effectively reduces ρ_c for the devices with low Si doping, while the ρ_c of the lightly doped diode with the highest S dose is reduced to a value close to that of the moderately doped diode with no S. This is an additional evidence that S is doping the junction. No improvement in ρ_c is observed for the degenerately doped diode by S implant since the initial dopant density is much higher than the extra dopant introduced by S. IPE measurements, shown in Figure 3(b), further confirm that the SBH is not reduced with S implant, remaining ~ 0.65 eV independent of S doses. Segregation of species other than S (e.g., Se, N, Sb, and Cl) are also reported to

drastically reduce the SBH to ~ 0.1 eV measured using a TE Arrhenius plot^{14–17} and may have the same TFE origin as in this report. Finally, the SBH extracted using TE has been observed to increase with S for NiSi/p-Si,¹ consistent with our explanation as the S could counter-dope the p-type substrate.

To ensure accurate extraction of the SBH, it is necessary to consider TFE when analyzing I - V data. Overall, the results suggest that implanted species such as S reduce the contact resistance of silicided junctions through a doping effect rather than true SBH lowering.

TABLE I. SBH measured with different techniques.

S (cm ⁻²)	Si (cm ⁻³)	SBH-Arrhenius (eV)	SBH – IPE (eV)	SBH – C-V (eV)
0	2×10^{15}	0.679	0.66	0.69
1×10^{13}	2×10^{15}	– ^a	0.65	0.70
5×10^{13}	2×10^{15}	– ^a	0.65	0.71
3×10^{14}	2×10^{15}	0.066	– ^b	0.58
0	5×10^{17}	–0.017	0.65	0.64

^aValues are not extracted since transport mechanism depends on temperature (refer to Figure 2).

^bValue is not extracted since photocurrent is lower than equipment detection limit.

¹S. M. Sze and K. K. Ng, *Physics of Semiconductor devices*, 3rd ed. (Wiley, Hoboken, 2007), Chap. 3, p. 187.

²Q. T. Zhao, U. Breuer, E. Rije, St. Lenk, and S. Mantl, *Appl. Phys. Lett.* **86**, 062108 (2005).

³E. Alptekin and M. Ozturk, *Microelectronics Eng.* **87**, 2358 (2010).

⁴H.-S. Wong, L. Chan, G. Samudra, and Y.-C. Yeo, *IEEE Electron Device Lett.* **28**, 703 (2007).

⁵Z. Zhang, Z. Qiu, R. Liu, M. Östling, and S.-L. Zhang, *IEEE Electron Device Lett.* **28**, 565 (2007).

⁶E. Alptekin and M. Ozturk, *IEEE Electron Device Lett.* **30**, 1272 (2009).

⁷T. P. Lee, K.-M. Tan, A. E.-J. Lim, H.-S. Wong, P.-C. Lim, D. M. Y. Lai, G.-Q. Lo, C.-H. Tung, G. Samudra, D.-Z. Chi, and Y.-C. Yeo, *Proceedings of IEDM*, 2006 851.

⁸S. Zhang and M. Ostling, *Crit. Rev. Solid State Mater. Sci.* **28**, 1 (2010).

⁹D. J. Coe and E. H. Rhoderick, *J. Phys. D* **9**, 965 (1976).

¹⁰M. Liehr, P. E. Schmid, F. K. LeGoues, and P. S. Ho, *Phys. Rev. Lett.* **54**, 19 (1985).

¹¹M. Tao, S. Agarwal, D. Udeshi, N. Basit, E. Maldonado, and W. P. Kirk, *Appl. Phys. Lett.* **83**, 2593 (2003).

¹²S. D. Brotherton, M. J. King, and G. J. Parker, *J. Appl. Phys.* **52**, 4649 (1981).

¹³H. G. Grimmeiss, E. Janzén, and B. Skarstam, *J. Appl. Phys.* **51**, 4212 (1980).

¹⁴H.-S. Wong, L. Chan, G. Samudra, and Y.-C. Yeo, *Appl. Phys. Lett.* **93**, 072103 (2008).

¹⁵P. Kalra, N. Vora, P. Majhi, P. Y. Hung, H.-H. Tseng, R. Jammy, and T.-J. K. Liu, *Electrochem. Solid-State Lett.* **12**, H1 (2009).

¹⁶H.-S. Wong, L. Chan, G. Samudra, and Y.-C. Yeo, *IEEE Electron Device Lett.* **28**, 1102 (2007).

¹⁷W.-Y. Loh, H. Etienne, B. Coss, I. Ok, D. Turnbaugh, Y. Spiegel, F. Torregrosa, J. Banti, L. Roux, P.-Y. Hung, J. Oh, B. Sassman, K. Radar, P. Majhi, H.-H. Tseng, and R. Jammy, *IEEE Electron Device Lett.* **30**, 1140 (2009).